JOURNAL OF MAGNETIC RESONANCE **125,** 28–33 (1997)
ARTICLE NO. MN961047

A Double-Modulation ESR Study of Internal Dynamics in the Glassy Polymer Matrix Detected by a Nitroxide Spin Probe

B. RAKVIN AND Z. VEKSLI

Ruder Bošković Institute, P.O. Box 1016, HR-10000, Zagreb, Croatia

Received July 1, 1996; revised October 14, 1996

The double-modulation ESR spin-probe technique was employed to study slow-motional dynamics in amorphous polymer matrices of polybutadiene, polyisobutylene, poly(methyl methacrylate), and paraffin. It was shown that the low-lying excitation levels of the polymer matrix, found in the range from 77 to 190 K below the internal spin-probe transition, affect the effective relaxation rate of a perdeuterated nitroxide probe. The interrelationship between the effective relaxation rates and the local molecular dynamics of side-chain groups attached to the polymer backbone was observed. Possible relaxation mechanisms are discussed within the electron–nuclear dipolar interaction. © 1997 Academic Press

INTRODUCTION

ESR spectroscopy of nitroxide spin probes has proved to provide very useful information about motional dynamics in different types of liquid, viscous, and glassy materials. Motional correlation times which are deduced from the rotational reorientations of spin probes can be found in a wide range, from 10^{-11} to 10^{-3} s^{-1} (*1, 2*). The extension of the spin-probe method to the region of slow-motional dynamics can offer better insight into the internal molecular motion in various solid-state matrices, which is of special interest.

In order to reach this goal, at least two additional experimental improvements to the conventional spin-probe method (*1*) should be more carefully considered. The first improvement is associated with the selection of the most suitable nitroxide probe possessing reduced intramolecular dynamics. Therefore, a perdeuterated spin probe having the motional dynamics of deuterated methyl groups in the slow-motion region significantly slower in comparison with a nondeuterated conventional probe is frequently employed. Second, one should avoid the problem of inhomogeneous broadening of the ESR line, which is usually found for a spin-probe spectrum near the rigid limit of molecular motion or for a highly restricted spin probe. One of the possible ways to avoid the problem of inhomogeneous line broadening is to measure the spin–spin relaxation time (T_2), spin–lattice relaxation time (T_1), or nuclear spin–lattice relaxation time (T_{N1}) of a probe (*1–3*). Since, for a spin probe in the slow-motion regime, the homogeneous linewidth ($1/T_2$) is larger than $1/T_1$, one can expect that the measurement of T_1 would make it possible to reach the smallest detectable local dynamical effects (approximately the same order of magnitude as $1/T_1$) which can be detected in the vicinity of a probe by the ESR-probe method (*4*).

In some cases it is also convenient to study an apparent spin–lattice relaxation time T_1^*, where $T_1^* \leqslant T_1$ (*4*), as an alternative way of approaching the complex dynamical behavior of a spin probe in the slow-motion region. This relaxation time is basically a T_1 slightly affected by some other dynamically sensitive relaxation process. For example, in the region near the rigid limit of the probe motion, one expects that the effect of intermolecular and intramolecular dynamics takes an important role in the process. However, recent measurements of T_1 by saturation recovery (*3*) show that less than ~10% of the influence on T_1 was due to intermolecular or intramolecular electron–nuclear couplings in the slow-motion region. Therefore, to gain more information from intramolecular and intermolecular relaxation processes, one can also study different types of T_1^* which would better reflect these effects.

As was shown earlier, a double-modulation ESR (DMESR) technique (*5*) can be used as an alternative method for detecting the T_1 of an inhomogeneously broadened line under the condition that $T_1 \gg T_2$ (*6–9*). Recently, it was also demonstrated that a modulation spectrum can be used for monitoring the slow-motional dynamics of a nitroxide spin probe (*10, 11*) and the internal free rotation of CH_3 groups attached to the piperidine ring of spin probes (*12*). In these studies, as well as in similar electron-spin-echo (ESE) studies (*4, 13–15*), it was noted that the spin probe exhibits a sharp change in the slope of a T_1^{DM} versus $1/T$ plot at about 190 K regardless of the polymer matrix and the probe (*12*). Therefore, we label this process the internal spin-probe transition. The spin-probe motion in the temperature region above the internal transition can be characterized by its rotational correlation time, while in the temperature region below the internal transition, it was assumed that the probe is nearly rigid and that the solid-state intramo-

1090-7807/97 $25.00

lecular and intermolecular relaxation process affects the T_1 and T_1^* values of a probe (*3, 4, 11*). Thus, by measuring T_1 or T_1^* of the perdeuterated probe in the temperature region below the internal transition, an optimum condition for detecting intermolecular dynamics around the nearly rigid probe in the matrix examined can be obtained.

One expects that polymers in glassy or in quasi-polycrystalline phase are among those systems where the spin probe is nearly rigid and where it can serve as a probe of internal motional dynamics in these matrices. The feasibility of detecting motional dynamics of various side groups which are attached to the main polymer chain in the glassy phase by employing a simple nitroxide spin probe will be the focus of the present work. The polymers containing side groups should exhibit a shorter relaxation time of the probe than the polymer chains without side groups. The temperature dependence of the backbone-chain relaxation times, and possible additional relaxation times corresponding to side-chain groups, will be related to the known spin–lattice relaxation mechanisms in the glassy matrix.

EXPERIMENTAL

The perdeuterated spin probe, 4-oxo-2,2,6,6-tetramethyl-1-piperidinyl-oxy (PD-Tempone), was dispersed in polymer matrices at low concentration where the dipolar linewidth broadening can be neglected (less than 0.02 mass %) (*16*). Four polymers differing in chain structure and side-chain groups, as well as corresponding relaxation modes, were selected: atactic poly(methyl methacrylate) (PMMA), $M_w = 4.4 \times 10^5$, and polyisobutylene (PIB), $M_w = 8.4 \times 10^5$, with two side-chain groups per molecular segment, and two polymers without side-chain groups, polybutadiene (PB), $M_w = 3 \times 10^3$, having random distribution of cis-1,4 and trans-1,4 structures, and paraffin 52/54.

DMESR measurements were performed on a Varian E-109 X-band spectrometer by using 100 kHz modulation of the Zeeman magnetic field as the first modulation. The second modulation (sweeping in the frequency interval from 250 to 350 kHz) was performed by an additional modulation coil and a Wavetek radiofrequency source. The modulation peak at 300 kHz was detected at a microwave power of less than 1 mW and accumulated in a standard PC computer. The linewidth at half-height of the DMESR peak, Δ_{obs}, is obtained by fitting a Lorentzian lineshape to the DMESR spectrum. Δ_{obs} is related to the spin–lattice relaxation time under the condition that $T_1 \gg T_2$ (*6, 7*):

$$1/\pi\Delta_{obs} = T_1^{DM} \sim T_1. \qquad [1]$$

The relation in Eq. [1] was tested by simultaneously detecting T_1 for paramagnetic centers in the irradiated quartz with pulsed ESR and DMESR techniques (*6*). The sensitivity of the DMESR method was recently demonstrated (*8*)

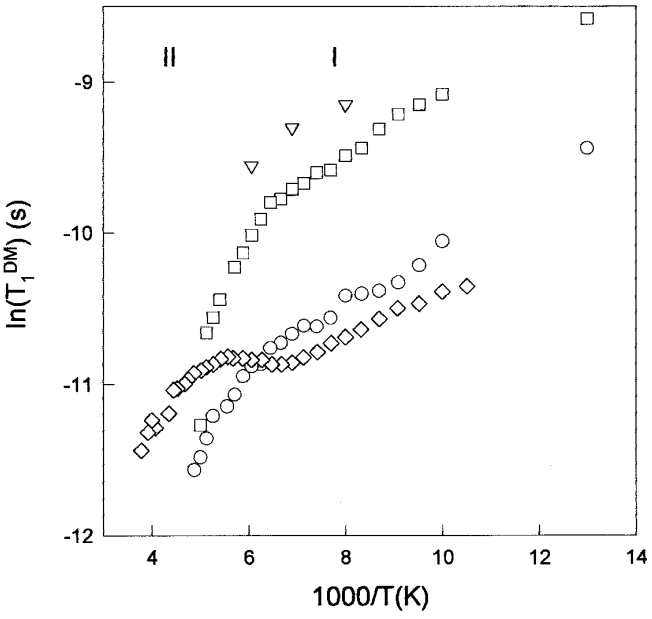

FIG. 1. DMESR linewidths represented as $\ln(T_1^{DM})$ vs inverse temperature for PD-Tempone dispersed in different polymer matrices: diamonds, PMMA; circles, PIB; squares, PB; and triangles, paraffin.

by T_1 measurements for AsO_4^{4-} in KH_2AsO_4. There is a good agreement with T_1 data obtained by the ESE method for the same radical center. Finally, the pulsed ESR and DMESR measurements on model systems, Tempone and PD-Tempone in a glycerol–water matrix, have been discussed in detail in our previous work (*11*), which shows that the T_1^{DM} can be approximated to the T_1^* values obtained by the stimulated-echo sequence. Since, in the following study, the contribution of the electron–nuclear dipolar, END, relaxation rate will be considered, it is interesting to test the sensitivity of T_1^{DM} to this particular relaxation mechanism. Following the results from Eaton and co-workers (*3*) on T_1, obtained by saturation recovery, one finds an ~10% difference between the T_1 of a deuterated and nondeuterated spin probe in a glycerol–water matrix at 100 K. The similar experiment performed earlier by DMESR (*11*) shows that T_1^{DM} is roughly of the same order of magnitude, but the difference between the deuterated and nondeuterated probe in the same matrix is about 90%. Thus, T_1^{DM} should detect an END type of relaxation with high sensitivity.

RESULTS AND DISCUSSION

The temperature dependence of T_1^{DM} for PD-Tempone dispersed in the matrices of four different polymers is shown in Fig. 1. The two distinct types of temperature behavior of the relaxation time can be clearly seen: the low-temperature region (from 77 to 190 K, denoted as I in Fig. 1) and the higher-temperature region (from 190 to 250 K, denoted as

TABLE 1
Fitted Coefficients, a, and Exponents, k, in the Temperature Region I

	$(T_1^{DM})^{-1} \propto aT^k$	
Matrix	a (K^{-k} s^{-1})	k
PB	1.8 ± 0.34	1.84 ± 0.05
PIB	75.2 ± 26.4	1.29 ± 0.07
PIB − PB	170 ± 99.1	1.03 ± 0.09

II). As discussed earlier for the various polymer matrices and different nitroxide probes (*12*), one expects an internal transition of the spin probe at temperatures around 190 K. The most prominent discrete relaxation processes in regions I and II are detected for the PB polymer matrix without side-chain groups. Above the internal spin-probe transition, a sharper change in the relaxation time can be ascribed to an increase in motional dynamics of the probe with a corresponding decrease in rotational correlation time. Below the internal transition, in region I, the probe is nearly rigid in motion and a smaller change in T_1^{DM} is detected. In this temperature region, T_1^{DM} should be affected only by the local dynamics in an amorphous polymer matrix. On comparing T_1^{DM} obtained for PB and T_1^{DM} obtained for a PIB polymer matrix in region I (Fig. 1), the shorter relaxation time for PIB than that for PB can be ascribed to the influence of the side-chain methyl groups on the PIB backbone. It can also be noted that the internal transition of PD-Tempone doped in the PIB matrix is not as well defined as in the PB matrix. However, at temperatures above the internal transition, both matrices exhibit comparable T_1^{DM}, as can be seen in Fig. 1. The temperature dependence of T_1^{DM} in the PMMA matrix indicates almost the same behavior as in the PIB matrix, with a slightly smaller value of T_1^{DM}. In order to confirm that the relaxation time in temperature region I is closely associated with the motional dynamics of polymer side-chain groups, we also measured a few values of T_1^{DM} for the paraffin matrix, which has polymer chains of a simple structure. The results shown in Fig. 1 are the longest relaxation times detected for PD-Tempone in the temperature region I. At region I temperatures, all the polymers are below the glass transition temperature, where polymer segmental motions are highly restricted (*17*). It has been postulated that, at temperatures below T_g, probe motion is largely independent of polymer-backbone motion and is determined by the static free volume of the polymer (*18*). The present experimental results clearly demonstrate that in the region below the internal transition of the nitroxide spin probe, a contribution to the spin–lattice relaxation time from the polymer local-mode relaxation, such as from side-chain groups, motional dynamics of very low activation energy can be detected by employing a perdeuterated probe and the DMESR technique.

Since proton dynamics from the side-chain groups in the polymer matrix modulate the electron spin–lattice relaxation rate, the possible underlying relaxation mechanisms will be discussed. Generally it is known that the spin–lattice relaxation for most free radicals trapped in a molecular crystal is dominated by two-phonon Raman processes at higher temperatures (~150 K) (*19*). It can be shown that when $T > \theta/2$ (θ is the Debye temperature), the Raman contribution to the relaxation rate is proportional to T^2. However, for a radical trapped in a glassy matrix, it was shown that the relaxation rate exhibits a linear temperature dependence (*19, 20*). These relaxation processes usually have their origin in the low-lying vibrational states and are often associated with the excitation of two-level systems, TLS. Thus, a rigid amorphous matrix can be tested on polycrystalline-type or glassy-type behavior by deducing the temperature dependence of the relaxation rate. From a log–log plot, the temperature dependence of $1/T_1^{DM}$ in region I and the exponents of the temperature dependence are obtained (Table 1). The experimental data and fitting curves are shown in Fig. 2. As expected, the observed relaxation rates are found to be between crystal- and glassy-type behavior. The amorphous polymer matrix containing side-chain methyl groups exhibits a smaller temperature exponent than the similar polymer matrix without the side groups. By comparing the PB and PIB matrices, which differ in side-chain groups attached to the polymer chain, it is possible to isolate the relaxation rate contribution corresponding to the motional dynamics of methyl groups. The results of the subtraction

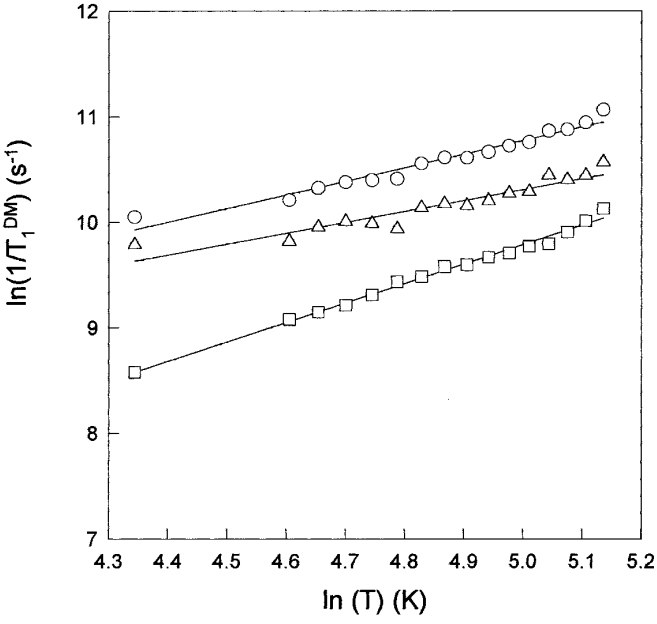

FIG. 2. ln–ln plot of the inverse of T_1^{DM} vs temperature for PD-Tempone dispersed in different matrices: circles, PIB; squares, PB; and triangles, differences, PIB − PB.

of relaxation rates of these two polymers (PIB − PB) and the corresponding fitting curve are also shown in the log–log plot in Fig. 2.

The temperature dependences for PIB and PB − PIB obtained exhibit nearly linear behavior in agreement with the theoretically predicted temperature dependence for a glassy-type matrix (*19, 20*). According to the model (*19–22*), the relaxation mechanism depends on the modulation of the END interaction between dispersed radicals and neighboring magnetic nuclei by tunneling modes or by TLS modes in the glassy matrix. It may also be noted that the coefficient of a relaxation process which varies linearly with temperature should be strongly affected by the number and distribution of these modes in the glassy matrix. Thus, an increase in the relaxation rate for the PIB polymer matrix in comparison to the PB matrix can be related to the expected increase in the local density of vibrational and TLS states in the system. It is important to note that, within experimental error, a linear temperature dependence of $1/T_1^{\mathrm{DM}}$ for extracted methyl groups is similar to that for $1/T_1$ measured for ethanol glasses up to high temperatures ($\sim$200 K) (*19*). Moreover, the coefficient $a = 170\ \mathrm{K}^{-k}\ \mathrm{s}^{-1}$, which is related to the density of tunneling and TLS modes in a glassy matrix, shows the same order of magnitude as the same type of coefficient obtained for a disordered matrix containing methyl groups ($a = 120\ \mathrm{K}^{-k}\ \mathrm{s}^{-1}$) (*23*). It should be noted that the polymer without side-chain groups, PB, shows a smaller linear contribution ($a \sim 2\ \mathrm{K}^{-1}\ \mathrm{s}^{-1}$) and larger exponent ($k = 1.84$) (Table 1), reflecting a more ordered solid than the polymer with side-chain groups.

The motional dynamics of the methyl groups in the PIB polymer matrix was studied earlier by NMR spectroscopy (*24, 25*). Near 140 K, a small fraction of the methyl groups rotate about their C_3 axes, while the others are interlocked. With an increase in temperature, it was found that the motional dynamics of CH_3 groups can be described better by a distribution of rotational correlation times than by a single correlation time. Since a distribution of correlation times for side-chain methyl groups is more appropriate for a glassy than for a crystalline environment, this may support the suggested relaxation mechanism (*21*) in the frozen PIB polymer matrix.

On the contrary, the contribution of TLS modes to the specific heat is usually expected only at temperatures an order of magnitude lower. However, in the earlier study (*19*), this discrepancy was explained by a possible stronger coupling between the spins and local TLS modes than between the spins and long-wavelength acoustic phonons. Another possible explanation of this discrepancy requires a closer and more critical examination of the nature of the detected relaxation rate, $1/T_1^{\mathrm{DM}}$, with regard to possible different types of proton END contributions. The experimental data on PMMA can be used as a good example for which both models can be applied, and this will be discussed below.

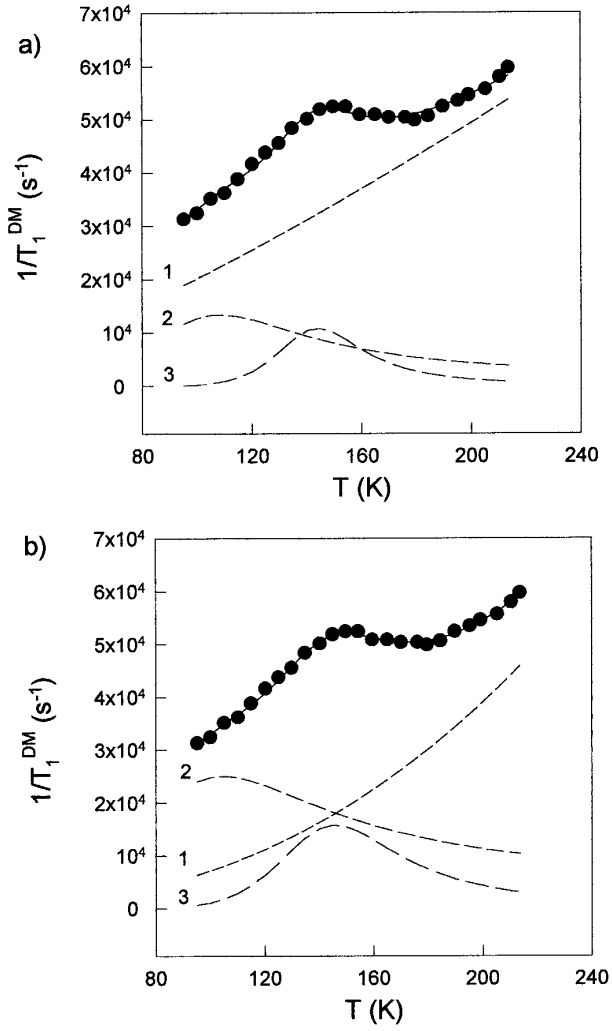

FIG. 3. DMESR linewidths represented as $1/T_1^{\mathrm{DM}}$ vs temperature for PD-Tempone dispersed in PMMA (solid circles). The dashed line 1 represents the contribution from the first term of Eq. [2], the dashed line 2 corresponds to the contribution of the electron-Larmor-frequency term, and the dashed line 3 is the contribution of the nuclear-Larmor-frequency term in Eq. [2]. The solid line is the sum of all contributions in relation [2]. (a) Fitted data with parameter $k = 1.29$. (b) Fitted data with parameter $k = 2.45$.

The spin-probe relaxation rates in glassy PMMA exhibit similar behavior and approximately the same value as in PIB (Fig. 1). However, the relaxation rate of PMMA exhibits a small maximum in the temperature region I (*27*) which is not found in the PIB matrix. The same data as in Fig. 1 for region I are replotted in Fig. 3 and reveal a clear maximum in the relaxation rate around 160 K. This behavior of the relaxation rate can be tentatively examined within the END relaxation mechanism. One expects an appearance of an extreme in the relaxation rate only when the rotational correlation times of the methyl protons reach values near $1/\omega_{\mathrm{n}}$ or $1/\omega_{\mathrm{e}}$, where ω_{n} represents the nuclear Larmor frequency and

TABLE 2
Fitted Coefficients from Eq. [2] for the PMMA Matrix in the Temperature Region I

Fit	k	a (K^{-k} s^{-1})	b (kHz)	τ_{01} (ps)	E_1 (kJ mol^{-1})	c (kHz)	τ_{02} (ps)	E_2 (kJ mol^{-1})	χ^2
I	1.29	53.0 ± 1.5	13.3 ± 0.9	0.32 ± 0.26	3.55 ± 0.61	10.9 ± 0.1	0.36 ± 0.28	12.4 ± 1.9	12.5
II	2.45	0.09 ± 0.004	25.1 ± 3.2	0.82 ± 0.46	2.61 ± 0.39	15.7 ± 2.7	7.24 ± 6.86	8.82 ± 1.13	5.6

ω_e represents the electron Larmor frequency. Therefore, the total relaxation rate for PMMA can be described by the END mechanism by combining TLS modes and classical orientational correlation times. This leads to the equation

$$\frac{1}{T_1^{DM}} = aT^k + b\left[\frac{2\omega_e\tau}{1+(\omega_e\tau)^2}\right] + c\left[\frac{2\omega_n\tau}{1+(\omega_n\tau)^2}\right], \quad [2]$$

where b and c represent a maximum of the relaxation rate due to proton END interaction and τ represents a rotational correlation time described by the Arrhenius equation, $\tau = \tau_0\exp(E/kT)$, with a temperature-independent activation energy E.

Equation [2] contains too many parameters for efficient fitting of the experimental results. Therefore, the data were fitted by choosing two arbitrary parameters for exponential temperature dependence which can be directly correlated with two different relaxation mechanisms. By assuming a relaxation mechanism similar to that for the spin probe doped in the PIB matrix, the exponent $k = 1.29$ was used as a fixed parameter. The best fit to Eq. [2] was obtained (Fig. 3a), and all the parameters, together with the corresponding errors and χ^2 error, are collected in Table 2. The contribution from the first term leads [dashed line (1) in Fig. 3a] to a linear coefficient $a = 53$ K^{-k} s^{-1} giving a good description of the glassy phase as found for the PIB polymer matrix (Table 1). The extreme behavior at lower temperatures with contribution coefficient $b = 13.3$ kHz is obtained for rapid proton motion with $\tau_{01} = 0.32$ ps and $E_1 = 3.5$ kJ/mol and by employing the electron Larmor frequency [dashed line (2) in Fig. 3a]. The extreme behavior at higher temperatures is described by the nuclear Larmor frequency and slower proton dynamics $\tau_{02} = 0.32$ ps and $E_2 = 12.4$ kJ/mol with contribution coefficient $c = 10.8$ kHz [dashed line (3) in Fig. 3a]. This model description leads to the two types of methyl-group dynamics in the observed temperature interval. One type of methyl group exhibits fast motional dynamics comparable to the electron Larmor frequency ($\omega_e^{-1} = 2.7 \times 10^{-11}$ s) while the second group performs slower motion comparable to the nuclear Larmor frequency ($\omega_n^{-1} = 1.8 \times 10^{-8}$ s). Earlier NMR (*28*) and recent neutron-scattering (*29*) measurements of the proton correlation time in PMMA also clearly show the two well-resolved types of motional dynamics corresponding to the faster ester side-chain methyl-group rotation with a smaller activation energy ($E \sim 0.7$ kJ/mol) and the slower main-chain methyl-group rotation with a larger activation energy ($E \sim 12$ kJ/mol).

In order to examine possible contributions from other possible relaxation mechanisms, different exponents in the first term were employed. The larger exponent ($k = 2.34 \pm 0.15$) than in the first fitting model is related to the spin–lattice relaxation rate detected for the probe in various glassy matrices by SR-ESR (*3*). Therefore, the parameter k was continuously increased until the minimum in the χ^2 error had been reached for the exponent $k = 2.45$. The corresponding fitted data are given in Table 2. In Fig. 3b, the solid line represents the best fit which is obtained from the three terms (represented as dashed lines) of Eq. [2]. Two major changes can be noted in the fitted parameters: a large decrease in a to 0.09 K^{-k} s^{-1} and an increase in b to 25.1 kHz. The consequence of this change is that the relaxation rate obtained from the first term in Eq. [2] coincides, within the experimental errors, with the experimentally detected $1/T_1$ for PD-Tempone in various glassy solvents (*3*), while the contribution of the faster ester methyl groups increases. The data obtained indicate that the relaxation rate detected by DMESR is significantly affected by the proton END interaction. In the recent description (*2*) of the direct measurement of the rotational correlation time, the mechanism of spin diffusion in which the matrix protons are coupled to the electrons and nuclei of a probe is presented in a form similar to the second and the third terms in Eq. [2]. These terms lead to maximum possible relaxation rates due to spin-diffusion mechanisms. The constants b and c obtained are well below the expected maximum diffusion rate (~130 kHz) for the PD-Tempol probe.

As shown for PB and PIB, a contribution of the side-group motion can be separated from the backbone dynamics. A TLS model description suggests that the first term, which describes the backbone dynamics, indicates more disordered glassy behavior (larger a and smaller k) of the PMMA matrix than that of the chains in the PB matrix. On the other hand, the same results described in terms of the proton-spin-diffusion relaxation model indicate a larger contribution to the relaxation rate in the matrix having the higher proton density and larger coupling END interactions. Larger proton density in PIB and PMMA than in the PB matrix could be responsible for the higher spin-diffusion contribution and the greater $1/T_1^{DM}$. In addition, the spin-diffusion contribu-

tions are strongly dependent on local proton dynamics, which can be seen in the different relaxation behaviors of PIB and PMMA.

CONCLUSIONS

There are a variety of techniques for measuring intramolecular dynamics in the slow-motion region. It is shown that, by employing a relatively simple method such as DMESR and a perdeuterated nitroxide spin probe, one can study slow-motional dynamics of a probe not only above the internal probe transition, as demonstrated and discussed in the previous papers (*11, 27*), but also in the region below this transition. The range of experimental information can be extended, due to the ability of the nitroxide probe to couple protons in the matrix and possible low-lying excitation levels of the matrix.

These experiments demonstrate that the measurements of T_1^{DM} for a perdeuterated spin probe dispersed in an amorphous polymer matrix can provide information about local motional dynamics. The values of $1/T_1^{DM}$ measured in selected polymer matrices are well below the expected maximum and can be related to an END relaxation mechanism. However, additional experimental measurements on the same model systems at lower temperatures as well as correlation with pulsed ESR and ENDOR measurements would be of considerable importance in order to fully characterize all the details of the $1/T_1^{DM}$ of the spin probe in the solid polymer matrix.

It is shown that local motional dynamics of side-chain groups are reflected as an increase in the effective relaxation rate of the probe. Proportionality between the density of TLS modes and other vibrational states with an increase in the effective relaxation rate can also be followed in these experiments. In addition, a temperature dependence of the effective relaxation rate can be used to elucidate the local molecular dynamics of the side-chain groups and the molecular packing of amorphous polymer chains due to their sequence. The experimental data obtained suggest that this method could offer valuable data on local dynamics and polymer chain packing of more complicated polymer systems such as block copolymers and polymer mixtures.

ACKNOWLEDGMENTS

The authors thank Dr. Y. Gallot for kindly providing the PB sample. The financial support of the Ministry of Science and Technology of the Republic of Croatia is acknowledged.

REFERENCES

1. L. J. Berliner (Ed.), ''Spin Labeling Theory and Application,'' Vols. 1 and 2, Academic Press, New York, 1976.
2. B. H. Robinson, D. A. Haas, and C. Mailer, *Science* **263,** 490 (1994).
3. J-L. Du, G. R. Eaton, and S. S. Eaton, *J. Magn. Reson. A* **115,** 213 (1995).
4. L. J. Schwartz, G. L. Millhauser, and J. H. Freed, *Chem. Phys. Lett.* **127,** 60 (1980).
5. B. Rakvin, T. Islam, and I. Miyagawa, *Phys. Rev. Lett.* **50,** 1313 (1983).
6. P. G. Below and A. D. Milov, *Chem. Phys. Lett.* **151,** 79 (1988).
7. B. F. Alekseev, A. B. Tikhonov, Yu. V. Bogachev, O. G. Gasimov, and V. A. Yanchurov, *Fiz. Tverd. Tela* **32,** 1305 (1980) [*Soviet Phys. Solid State* **32,** 764 (1980)].
8. B. Rakvin, *J. Magn. Reson. A* **106,** 245 (1994).
9. B. Rakvin, and N. S. Dalal, *Phys. Rev. B* **49,** 13211 (1994).
10. B. Rakvin, *Chem. Phys. Lett.* **109,** 280 (1984).
11. B. Rakvin, S. Valić, and Z. Veksli, *Chem. Phys. Lett.* **182,** 171 (1991).
12. S. Valić, B. Rakvin, Z. Veksli, and S. Pečar, *Chem. Phys. Lett.* **199,** 609 (1992).
13. L. J. Schwartz, A. E. Stillman, and J. H. Freed, *J. Chem. Phys.* **77,** 5410 (1982).
14. G. L. Millhauser and J. H. Freed, *J. Chem. Phys.* **81,** 37 (1984).
15. S. A. Dzuba, A. G. Maryasov, K. M. Salikhov, and Yu. D. Tsvetkov, *J. Magn. Reson.* **58,** 95 (1984).
16. Z. Veksli, B. Rakvin, M. Andreis, Z. Grubišić-Gallot, and P. Lutz, *Makromol. Chem., Rapid Commun.* **7,** 691 (1986).
17. J. D. Ferry, ''Viscoelastic Properties of Polymers,'' Wiley, New York, 1979.
18. G. G. Cameron, *in* ''Comprehensive Polymer Science'' (A. Alen and J. C. Berington, Eds.), Vol. 1, Pergamon Press, Oxford, 1989.
19. M. K. Bowman and L. Kevan, *in* ''Time Domain Electron Spin Resonance'' (L. Kevan and R. N. Schwartz, Eds.), Wiley, New York, 1979.
20. J. Kurtz and H. J. Stapleton, *Phys. Rev. B* **22,** 2195 (1980).
21. M. K. Bowman and L. Kevan, *J. Phys. Chem.* **81,** 456 (1977).
22. H. Thomann, L. R. Dalton, and L. A. Dalton, *in* ''Biological Applications of Time Domain ESR, Biological Magnetic Resonance 6'' (L. J. Berliner and J. Reuben, Eds.), Plenum Press, New York, 1984.
23. J. M. Michalik and L. Kevan, *J. Chem. Phys.* **68,** 5325 (1978).
24. J. G. Powles, *Proc. Phys. Soc. (London) B* **69,** 281 (1956).
25. A. W. Nolle and J. J. Billings, *J. Chem. Phys.* **30,** 84 (1959).
26. A. Nittke, M. Scherl, P. Esquinazi, W. Lorenz, Juanyun Li, and F. Pobell, *J. Low. Temp. Phys.* **98,** 517 (1995).
27. S. Valić, B. Rakvin, Z. Veksli, and Z. Grubišić-Gallot, *Macromolecules* **23,** 5182 (1990).
28. J. G. Powles, B. I. Hunt, and D. J. H. Sandiford, *Polymer* **5,** 505 (1964).
29. G. Floudas and J. S. Higgins, *Polymer* **33,** 4121 (1992).